



A Novel Algorithm for Heart Rate Estimation Based on Synchrosqueezing Transform

Nils Laurent, Sylvain Meignen, Julie Fontecave-Jallon, Bertrand Rivet

► To cite this version:

Nils Laurent, Sylvain Meignen, Julie Fontecave-Jallon, Bertrand Rivet. A Novel Algorithm for Heart Rate Estimation Based on Synchrosqueezing Transform. EUSIPCO 2021 - 29th European Signal Processing Conference, Aug 2021, Dublin, Ireland. pp.1286-1290, <10.23919/EUSIPCO54536.2021.9616306>. <hal-03544794>

HAL Id: hal-03544794

<https://hal.science/hal-03544794v1>

Submitted on 1 Apr 2022

HAL is a multi-disciplinary open access archive for the deposit and dissemination of scientific research documents, whether they are published or not. The documents may come from teaching and research institutions in France or abroad, or from public or private research centers.

L'archive ouverte pluridisciplinaire **HAL**, est destinée au dépôt et à la diffusion de documents scientifiques de niveau recherche, publiés ou non, émanant des établissements d'enseignement et de recherche français ou étrangers, des laboratoires publics ou privés.



HAL Authorization

A Novel Algorithm for Heart Rate Estimation Based on Synchrosqueezing Transform

Nils Laurent, Sylvain Meignen

Jean Kuntzmann Laboratory

University Grenoble Alpes

Grenoble, France

nils.laurent1@univ-grenoble-alpes.fr

sylvain.meignen@univ-grenoble-alpes.fr

Julie Fontecave-Jallon

TIMC-IMAG Laboratory

University Grenoble Alpes

Grenoble, France

julie.fontecave@univ-grenoble-alpes.fr

Bertrand Rivet

GIPSA-Lab

University Grenoble Alpes

Grenoble, France

bertrand.rivet@gipsa-lab.grenoble-inp.fr

Abstract

To estimate the heart rate (HR) from electrocardiogram (ECG), time-frequency representations such as the short-time Fourier transform (STFT) is often used. As the STFT is constrained by the choice of a specific analysis window used for its definition, we alternatively propose to estimate HR from a synchrosqueezed STFT. More precisely, we build a novel algorithm inspired by non-negative matrix factorization to estimate HR by determining the minimal Wasserstein distance between a synchrosqueezed STFT and columns of a specific dictionary matrix. Throughout numerical simulations carried out on both synthetic and real ECGs, we show in what way to use a synchrosqueezed STFT rather than STFT improves HR estimation.

Index Terms

HR estimation, non-negative matrix factorization, Wasserstein distance, synchrosqueezing transform.

I. INTRODUCTION

HR estimation from electrocardiogram (ECG) recordings has been a very active research topic in the past decades, and can be either signal-based, as for instance in techniques using R-peak detection [1], [2], or *time-frequency* (TF) based [3], [4]. TF analysis has been used on ECG signals in many different circumstances as for instance to detect abnormal behaviors like sleep apnea [5], to study arrhythmia [6], to identify coronary artery diseases [7] or to separate fetal ECG from that of the mother [8]. Regarding this last application, there exist many other alternative techniques to extract fetal ECG among which one may cite blind source separation [9], [10], blind adaptive filtering [11], Kalman filter [12], to name but a few.

In the present paper, the focus is put on TF-based HR estimation and, more precisely, we investigate the STFT of ECGs. In that context, the basic principle ruling HR estimation is that an ECG corresponds at each time instant to the sum of several harmonics whose frequencies are multiples of the so-called *fundamental frequency* (FF) which is the sought HR. For its estimation, we first propose to compare STFT at each time instant with the columns of a dictionary matrix, being aware that such an approach will necessarily be constrained by the choice of the window used in STFT definition. To cope with this issue, we carry out the same approach but using the reassigned STFT named *synchrosqueezing transform* (FSST) instead of STFT. The rationale to consider such a *time-frequency representation* (TFR) is that we believe the reassignment process, by sharpening the TFR it is based on, should lead to a more accurate HR estimation. Note that the synchrosqueezing transform was first introduced to reassign the continuous wavelet transform [13] and then extended to STFT reassignment in [14], [15]. As FSST reassigns exactly only signals made of pure harmonics, an extension of FSST was introduced to deal with more frequency modulated signals [16], called FSST2. In this regard, we will therefore investigate whether to use FSST2 instead of FSST also brings some improvements in terms of HR estimation.

The paper is organized as follows: in Section II, we recall some basic definitions on STFT, synchrosqueezing transforms, and *non-negative matrix factorization* (NMF) and then detail our novel algorithm, inspired by NMF, that uses either STFT or its reassigned versions to perform HR estimation, in Section III. Numerical results on both simulated and real ECG signals conclude the paper.

II. DEFINITIONS

A. Time frequency Analysis

Considering a signal $f \in L^1(\mathbb{R}) \cap L^2(\mathbb{R})$ and a real window $g \in L^\infty(\mathbb{R}) \cap L^2(\mathbb{R})$, its STFT is defined as:

$$V_f^g(t, \eta) = \int_{\mathbb{R}} f(\tau) g(\tau - t) e^{-2i\pi(\tau - t)\eta} d\tau. \quad (1)$$

This work was supported in part by the University Grenoble Alpes under IRS Grant "AMUSETE" and the ANR ASCETE project with grant number ANR-19-CE48-0001-01.

In this paper, we assume ECG is modeled by a specific kind of *multicomponent signals* (MCSs):

$$f(t) = \sum_{p=1}^P A_p(t) e^{2i\pi p\phi'(t)}, \quad (2)$$

where ϕ' is the fundamental frequency (FF) and A_p the *instantaneous amplitude* (IA).

B. Synchrosqueezing Transforms

While STFT is very commonly used to analyze signals of type (2), it is constrained by the Heisenberg uncertainty principle that stipulates that STFT cannot be perfectly localized in time and frequency at the same time. Therefore, the choice of the analysis window g is central in that context.

To improve the TF localization of STFT, different reassignment techniques were introduced among which FSST [14], [15] is one of the most popular. In a nutshell, using the local instantaneous frequency estimator given by a reassignment operator

$$\hat{\omega}(t, \eta) = \Re\{\tilde{\omega}(t, \eta)\} \text{ with } \tilde{\omega}(t, \eta) = \eta - \frac{1}{2i\pi} \frac{V_f^{g'}(t, \eta)}{V_f^g(t, \eta)},$$

where $\Re\{X\}$ is the real part of complex number X . FSST reassigns STFT coefficients with modulus larger than a threshold λ through:

$$T_f^\lambda(t, \omega) = \int_{|V_f^g(t, \eta)| > \lambda} V_f^g(t, \eta) \delta(\omega - \hat{\omega}(t, \eta)) d\eta. \quad (3)$$

A discrete time and frequency version of the synchrosqueezing transform given by (3) can then be derived, corresponding to a $K \times N$ matrix, N being the length of the signal and K the number of frequency bins.

Since FSST is unable to properly reassign MCSs containing frequency modulated modes, an extension was proposed to deal with this issue through the so-called *second order synchrosqueezing transform* (FSST2) [14], [16]. The latter is defined by means of the second order local complex IF estimate of f [16]:

$$\tilde{\omega}^{(2)}(t, \eta) = \begin{cases} \tilde{\omega}(t, \eta) + \tilde{q}(t, \eta)(t - \tilde{t}(t, \eta)) & \text{if } \partial_t \tilde{t}(t, \eta) \neq 0 \\ \tilde{\omega}(t, \eta) & \text{otherwise,} \end{cases}$$

in which: $\tilde{t}(t, \eta) = t + \frac{V_f^{tg}(t, \eta)}{V_f^g(t, \eta)}$, and $\tilde{q}(t, \eta) = \frac{1}{2i\pi} \frac{V_f^{g''}(t, \eta)V_f^g(t, \eta) - (V_f^{g'}(t, \eta))^2}{V_f^{tg}(t, \eta)V_f^{g'}(t, \eta) - V_f^{tg'}(t, \eta)V_f^g(t, \eta)}$. Finally, $\hat{\omega}^{(2)}(t, \eta) = \Re\{\tilde{\omega}^{(2)}(t, \eta)\}$ corresponds to the desired local IF estimate. FSST2 is then defined by replacing $\hat{\omega}$ by $\hat{\omega}^{(2)}$ in (3). In the same way as for FSST, a discrete time and frequency version of FSST2 can be derived.

C. NMF Basics

Non-negative matrix factorization (NMF) decomposes a given non-negative data matrix $\mathbf{X} \in \mathbb{R}^{K \times N}$ into two non-negative matrices, the *dictionary matrix* $\mathbf{W} \in \mathbb{R}^{K \times K_e}$ and the *activation matrix* $\mathbf{H} \in \mathbb{R}^{K_e \times N}$ such that $\mathbf{X} \approx \mathbf{WH}$, K_e being the number of components in the dictionary. The decomposition is based on minimizing the reconstruction error of \mathbf{X} through \mathbf{WH} , which can be formulated as [17]

$$\min_{\mathbf{W}, \mathbf{H}} D(\mathbf{X}|\mathbf{WH}) \text{ subject to } \mathbf{W} \geq 0, \mathbf{H} \geq 0. \quad (4)$$

The most popular cost functions D are the Euclidean distance, Kullback-Leibler (KL) divergence and Itakura-Saito (IS) distance. To solve the problem defined in (4), a maximization-minimization algorithm based on multiplicative updates [17] is widely used [18].

D. Definition of the Dictionary Matrices

In the context of ECG signals analysis, we consider a fixed dictionary \mathbf{W} , in which each column corresponds to a specific *fundamental frequency* (FF). In the following study, we will consider that \mathbf{X} is either STFT (see an illustration in Fig. 1 (a)), FSST or FSST2 moduli (see an illustration in Fig. 1 (b) for FSST2). Taking into account that, for resting patients, FF may vary between 30 and 180 beats per minute (bpm), when \mathbf{X} is either FSST or FSST2 moduli, we consider the dictionary matrix given in Fig. 1 (d), which we denote by \mathbf{W}^0 . This matrix consists of K_e columns corresponding to 151 components each of which corresponds to an integer FF between 30 and 180 bpm. The coefficients in each column are set to one when they correspond to multiples of FF, and zero elsewhere. With such a dictionary matrix, only some of the harmonics are taken into account, since fewer harmonics are present in \mathbf{W}^0 when FF increases. Furthermore, the fact that the different harmonics have different amplitude is not considered. We will see that these aspects do not much alter HR estimation performance with the algorithm we propose.

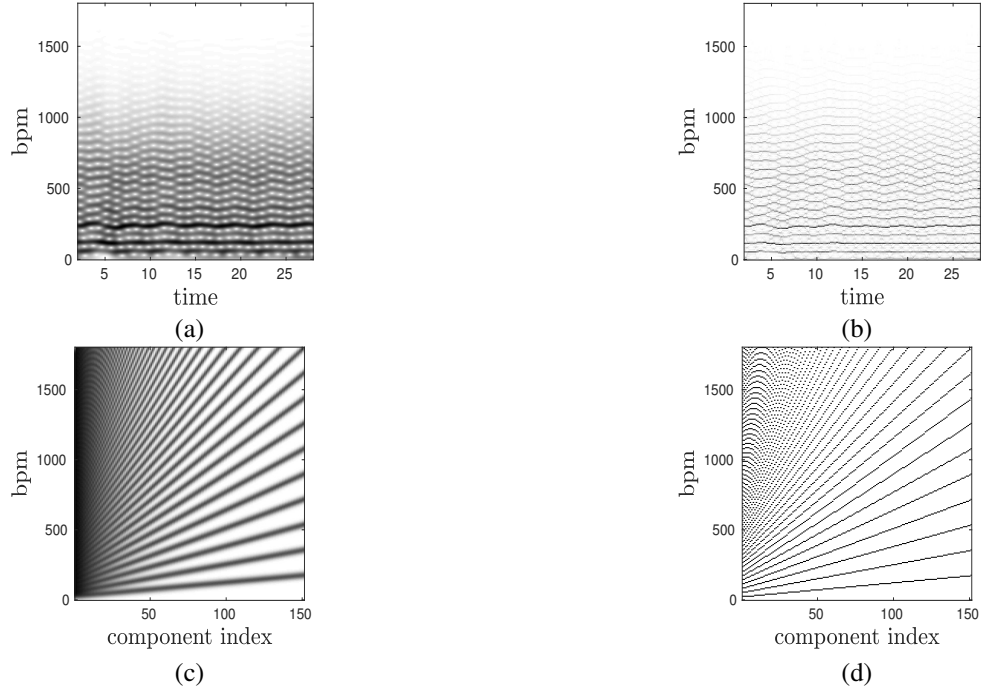


Fig. 1. (a): STFT of an ECG generated following [19]; (b): FSST2 of the same ECG; (c): Dictionary matrix \mathbf{W}^1 used with STFT-based approach; (d): Dictionary matrix \mathbf{W}^0 used with FSST2-based approach. For the sake of legibility, in (c) and (d) we do not normalize the column of the matrices.

When \mathbf{X} corresponds to STFT modulus, one has to take into account the width of the analysis window in the definition of the dictionary matrix. For the sake of simplicity, we here consider a Gaussian window of the form $e^{-\pi \frac{x^2}{\sigma^2}}$. In the Fourier domain, it corresponds to $e^{-\pi \sigma^2 \eta^2}$. So, to build the dictionary in the STFT case, we consider a simple convolution of each column of \mathbf{W}^0 with $e^{-\pi \sigma^2 \eta^2}$. This results in the dictionary matrix denoted by \mathbf{W}^1 (see Fig. 1 (c)).

III. NMF-LIKE DECOMPOSITION BASED ON FSST MAGNITUDE

A. Computation of Activation Matrix Using Wasserstein Distance

With a fixed dictionary matrix, the computation of \mathbf{H} when D is the Euclidian distance boils down to a simple least-square minimization problem:

$$\mathbf{H} = \underset{\mathbf{H}_0}{\operatorname{argmin}} \|\mathbf{X} - \mathbf{W}\mathbf{H}_0\|^2,$$

and thus \mathbf{H} satisfies $\mathbf{W}^T \mathbf{W} \mathbf{H} = \mathbf{W}^T \mathbf{X}$, and is not necessarily unique. Alternatively, we impose that \mathbf{H} be associated with only one function in the dictionary, and we compute \mathbf{H} by minimizing, at each time instant, a specific *earth mover distance* (EMD) [20]. Let us recall that EMD is a sliced Wasserstein distance that aims at comparing probability distributions, and that it has already been used in the TF context for instance in [16], [21]–[23].

We propose to compute the sliced Wasserstein distance d between \mathbf{X} at time n , corresponding to the column \mathbf{X}_n of \mathbf{X} (normalized by its sum so that it can be viewed as a probability distribution) and each column of the matrix \mathbf{W} , the i^{th} column of \mathbf{W} being denoted by \mathbf{W}_i (normalized by its sum), and then define

$$i_0 = \underset{i}{\operatorname{argmin}} d(\mathbf{W}_i, \mathbf{X}_n). \quad (5)$$

Finally, \mathbf{H}_n , the n^{th} column of \mathbf{H} , is such that $\mathbf{H}_{i,n} = 0$ if $i \neq i_0$, and $\mathbf{H}_{i_0,n} = 1$.

B. Algorithm for HR Computation

The approach we propose for HR estimation is based on minimal Wasserstein and consists of several steps.

First, one defines a probability of false HR detection on a test signal. To do so, we first estimate the mean HR i_M by the median of the component indices associated with the minimal Wasserstein distance over the whole test signal duration. Let

us denote by \hat{i}_M this estimate. To measure good detections, we consider the interval $\hat{I} = [\frac{3\hat{i}_M}{4}, \frac{3\hat{i}_M}{2}]$, and then define \hat{B} as follows:

$$\hat{B} = \frac{\#\{n, \underset{i}{\operatorname{argmin}} d(\mathbf{W}_i, \mathbf{X}_n) \in \hat{I}\}}{N}. \quad (6)$$

The rationale supporting the definition of \hat{I} is that the largest sub-harmonic is located at $\frac{\hat{i}_M}{2}$ and the smallest harmonic at $2\hat{i}_M$, and thus \hat{I} corresponds to the half intervals between these and FF. The probability of false detection is then defined as $P_f = 1 - \hat{B}$.

Assuming P_f is known, the first step of the proposed HR estimation for a given ECG signal consists of computing n_{med} an estimate of the minimal time index such that the probability that the median of the detection computed from time indices 1 to n_{med} is exact with probability p_0 . Assuming the locations of false detections are randomly distributed, n_{med} can be computed using the binomial law as follows:

$$n_{med} = \underset{n}{\operatorname{argmin}} \left(\sum_{k=0}^{n/2} C_n^k P_f^k (1 - P_f)^{n-k} \leq p_0 \right). \quad (7)$$

Knowing n_{med} , we compute HR estimates for time indices between 1 and n_{med} , following the scheme described in Algorithm 1. To check a posteriori the validity of the computed n_{med} , we compute the median of the detection between time indices 1 and n_{med} , and then recompute an estimate of \hat{B} from this set using the same approach as before. If \hat{B} is lesser than $1 - \beta P_f$ (β is fixed to $3/4$ here) n_{med} is increased until \hat{B} becomes larger than $1 - \beta P_f$. Having defined HR estimation for the first n_{med} time indices, the estimation carries on following the approach described in Algorithm 2, in which γ is some parameter whose influence will be discussed in the Results section.

Algorithm 1: HR estimation step 1

Input : $\mathbf{W}, \mathbf{X}, n_{med}$
for $n = 1, \dots, n_{med}$ **do**
 $\tilde{\mathbf{i}}[n] = \underset{i \in [1, K_e]}{\operatorname{argmin}} d(\mathbf{W}_i, \mathbf{X}_n)$
end
 $i_M = \operatorname{median} \{ \tilde{\mathbf{i}}[n], n = 1, \dots, n_{med} \}$
for $n = 1, \dots, n_{med}$ **do**
 $\hat{\mathbf{i}}[n] = \underset{i \in [\frac{3}{4}i_M, \frac{3}{2}i_M]}{\operatorname{argmin}} d(\mathbf{W}_i, \mathbf{X}_n)$
end

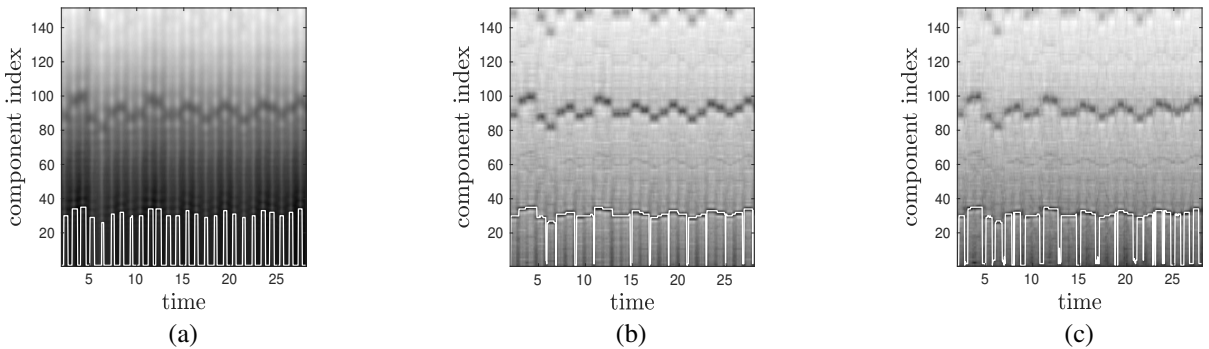


Fig. 2. (a): modulus of STFT, the white curve corresponds to the indices associated with the minimal Wasserstein distance ($\hat{B} = 39.61\%$); (b): same as (a) but for FSST ($\hat{B} = 94.34\%$) (c): same as (a) but for FSST2 ($\hat{B} = 75.4\%$).

It is worth noting here that to improve the computational efficiency of the proposed algorithm we compute only the Wasserstein distance on a small number of elements of the dictionary.

IV. RESULTS

In this section, we first investigate false detections depending on the TFR used to compute \hat{B} , then we explain how to fix the parameter γ in Algorithm 2 by studying the behavior of this algorithm on synthetic ECG generated by the MATLAB function

Algorithm 2: HR estimation step 2

Input : $\mathbf{W}, \mathbf{X}, n_{med}, \hat{\mathbf{i}}[1, \dots, n_{med}], \gamma$
for $n = n_{med} + 1, \dots, L$ **do**
 $\Delta_n = \text{std} \left\{ \hat{\mathbf{i}}[k], k = 1, \dots, n - 1 \right\}$
 $\hat{\mathbf{i}}[n] = \underset{[\hat{\mathbf{i}} - \gamma \Delta_n, \hat{\mathbf{i}} + \gamma \Delta_n]}{\text{argmin}} \quad d(\mathbf{W}_i, \mathbf{X}_n)$
end

HR Mean	\hat{B} STFT	\hat{B} FSST	\hat{B} FSST2
60 bpm	39.61%	94.34%	75.4%
70 bpm	81.18%	99.14%	90.04%
80 bpm	100%	100%	100%

TABLE I

COMPUTATION OF \hat{B} ON SYNTHETIC ECG SIGNALS WITH DIFFERENT HR MEANS WHEN EITHER STFT, FSST OR FSST2 ARE USED TO COMPUTE \mathbf{X}

”ecgsyn” developed in [19]. Finally, we conclude by showing some results on real ECGs extracted from the SiSEC database [24].

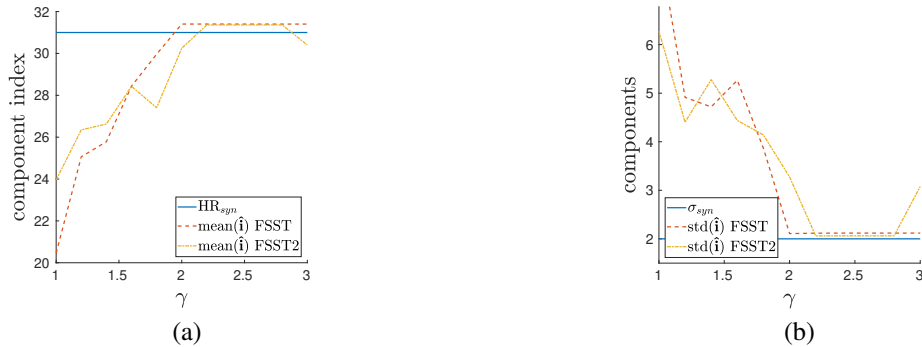
A. Determination of the Probability of False Detection

To compare the different probability of false detection depending on the type of TFR used to define \mathbf{X} , we consider synthetic ECGs generated as in [19], compute the corresponding STFT, FSST, and FSST2 and then (5) for each time instant when \mathbf{X} is associated with one of the just mentioned TFRs. With these synthetic signals, the mean HR component i_M is known, and we measure good detection by considering $I = [\frac{3i_M}{4}, \frac{3i_M}{2}]$ and then

$$B = \frac{\#\{n, \underset{i}{\text{argmin}} d(\mathbf{W}_i, \mathbf{X}_n) \in I\}}{N}, \quad (8)$$

the probability of false detection being $1 - B$. We numerical notice that, with STFT or FSST2 the minimum of the Wasserstein distance is much more likely to be associated with a sub-harmonic than when FSST is used, resulting in a much higher probability of false detection, and this is true whatever the mean HR (the results are depicted in Table. I). An illustration of this is given in Fig. 2 (a)-(c) when the TFR are either STFT, FSST and FSST2, respectively: the white curves correspond to the indices associated with the minimal Wasserstein distance for each time index n . We notice that false detections usually occur when HR changes rapidly, and, as the signal is quasi-harmonic, to make a linear chirp approximation on the modes, as is done in FFST2, results in error at these time indices. As our plan is to use Wasserstein distance for HR computation, we will make use of FSST rather than STFT or FSST2.

B. Determination of γ on Synthetic ECG

Fig. 3. (a): Estimation of HR mean from $\hat{\mathbf{i}}$. (b): Estimation of the corresponding standard deviation.

The goal of this section is to define an appropriate choice for parameter γ used in Algorithm 2. For that purpose, we investigate how good this algorithm is to estimate the mean and standard deviation of HR, which are input parameters of the

function "ecgsyn". In what follows, we denote by HR_{syn} the mean heart rate and by σ_{syn} its standard deviation. To make HR estimation realistic we consider $HR_{syn} = 60$ bpms (corresponding to component index 31) and $\sigma_{syn} = 2$ bpms. Such a signal enables a clear separation between harmonics and enough variability of HR, so that its study is useful for the analysis of real ECGs that comes next. For that type of signals, we compute the mean of \hat{i} along with its standard deviation, expressed in terms of a number of components, both as a function of γ . The results depicted in Fig. 3 (a) and (b) show that the proposed algorithm enables very accurate estimations of both the mean and standard deviation of HR provided γ is taken around 2.5. Note that the range for γ to retrieve the mean and standard deviation of HR is very similar when either FSST or FSST2 is considered.

C. Study of Real ECGs

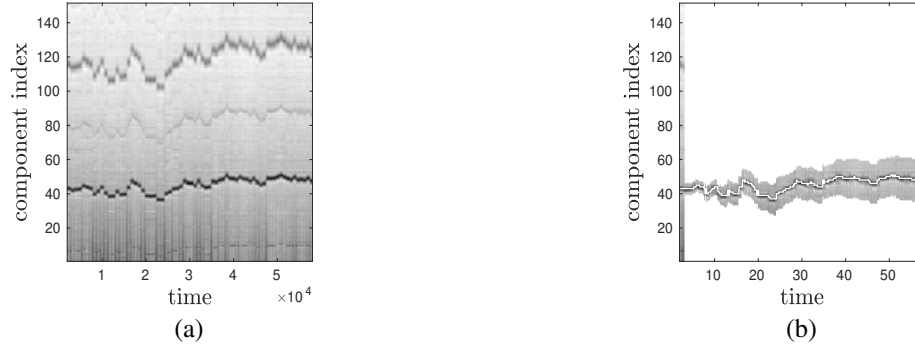


Fig. 4. (a) FSST based EMD of a real ECG signal. (b) HR detection on the same signal using $\gamma = 3$.

We here study ECGs extracted from SiSEC database [24], which correspond to thoracic recordings, which can be contaminated by different types of noises, and in particular impulse noises. EMD based on FSST computed on such a signal, and γ fixed as explained in Section IV-B, is depicted in Figure 4 (a). The presence of impulsive noises tends to create some local minima of the Wasserstein distance at frequencies corresponding to the largest sub-harmonic of the true FF. As FSST somehow reduces the noise while enhances the significant harmonics, the proposed HR estimation algorithm never gets trapped by minima that arise at sub-harmonic locations. We display in Fig. 4 (b) \hat{i} (white line) along with the TF region corresponding to standard deviation Δ_n , when n varies.

V. CONCLUSION

In this paper, we have introduced a novel procedure for HR estimation from the reassigned time-frequency representation of ECG recordings. The proposed approach has been developed on the time-frequency representation associated with the synchrosqueezing transform of the short-time Fourier transform. The simulations carried out on synthetic ECGs help us finding the most appropriate TFR for HR estimation and the right parameters values. An application to real ECG signals was then proposed, for which promising results were derived. In a near future, we plan to extend this approach to more complex situations principally the monitoring of fetal activity, to study more in detail the impact of noise on the proposed HR estimate, and also to investigate how to use the proposed algorithm for abnormal behavior detection like arrhythmia or sleep apnea.

REFERENCES

- [1] Jiapu Pan and Willis J Tompkins, "A real-time qrs detection algorithm," *IEEE transactions on biomedical engineering*, , no. 3, pp. 230–236, 1985.
- [2] Daniel T Kaplan, "Simultaneous qrs detection and feature extraction using simple matched filter basis functions," in *[1990] Proceedings Computers in Cardiology*. IEEE, 1990, pp. 503–506.
- [3] Jingshan Huang, Binqiang Chen, Bin Yao, and Wangpeng He, "Ecg arrhythmia classification using stft-based spectrogram and convolutional neural network," *IEEE Access*, vol. 7, pp. 92871–92880, 2019.
- [4] Basheeruddin Shah Shaik, GVSSKR Naganjaneyulu, T Chandrasheker, and AV Narasimhadhan, "A method for qrs delineation based on stft using adaptive threshold," *Procedia Computer Science*, vol. 54, pp. 646–653, 2015.
- [5] AF Quiceno-Manrique, JB Alonso-Hernandez, CM Travieso-Gonzalez, MA Ferrer-Ballester, and G Castellanos-Dominguez, "Detection of obstructive sleep apnea in ecg recordings using time-frequency distributions and dynamic features," in *2009 Annual International Conference of the IEEE Engineering in Medicine and Biology Society*. IEEE, 2009, pp. 5559–5562.
- [6] Safa Sultan Qurraie and Rashid Ghorbani Afkhami, "Ecg arrhythmia classification using time frequency distribution techniques," *Biomedical engineering letters*, vol. 7, no. 4, pp. 325–332, 2017.
- [7] Manish Sharma and U Rajendra Acharya, "A new method to identify coronary artery disease with ecg signals and time-frequency concentrated antisymmetric biorthogonal wavelet filter bank," *Pattern Recognition Letters*, vol. 125, pp. 235–240, 2019.
- [8] Li Su and Hau-Tieng Wu, "Extract fetal ecg from single-lead abdominal ecg by de-shape short time fourier transform and nonlocal median," *Frontiers in Applied Mathematics and Statistics*, vol. 3, pp. 2, 2017.
- [9] Lieven De Lathauwer, Bart De Moor, and Joos Vandewalle, "Fetal electrocardiogram extraction by blind source subspace separation," *IEEE transactions on biomedical engineering*, vol. 47, no. 5, pp. 567–572, 2000.

- [10] Mahsa Akhbari, Mohammad Niknazar, Christian Jutten, Mohammad B Shamsollahi, and Bertrand Rivet, "Fetal electrocardiogram r-peak detection using robust tensor decomposition and extended kalman filtering," in *Computing in Cardiology 2013*. IEEE, 2013, pp. 189–192.
- [11] D Graupe, MH Graupe, Y Zhong, and RK Jackson, "Blind adaptive filtering for non-invasive extraction of the fetal electrocardiogram and its non-stationarities," *Proceedings of the Institution of Mechanical Engineers, Part H: Journal of Engineering in Medicine*, vol. 222, no. 8, pp. 1221–1234, 2008.
- [12] Mohammad Niknazar, Bertrand Rivet, and Christian Jutten, "Fetal ecg extraction by extended state kalman filtering based on single-channel recordings," *IEEE Transactions on Biomedical Engineering*, vol. 60, no. 5, pp. 1345–1352, 2012.
- [13] Ingrid Daubechies, Jianfeng Lu, and Hau-Tieng Wu, "Synchrosqueezed wavelet transforms: an empirical mode decomposition-like tool," *Applied and Computational Harmonic Analysis*, vol. 30, no. 2, pp. 243–261, 2011.
- [14] T. Oberlin, S. Meignen, and V. Perrier, "The Fourier-based synchrosqueezing transform," in *2014 IEEE International Conference on Acoustics, Speech and Signal Processing (ICASSP)*, May 2014, pp. 315–319.
- [15] Gaurav Thakur, Eugene Brevdo, Neven S. FućKar, and Hau-Tieng Wu, "The synchrosqueezing algorithm for time-varying spectral analysis: Robustness properties and new paleoclimate applications," *Signal Processing*, vol. 93, no. 5, pp. 1079–1094, May 2013.
- [16] Ratikanta Behera, Sylvain Meignen, and Thomas Oberlin, "Theoretical analysis of the second-order synchrosqueezing transform," *Applied and Computational Harmonic Analysis*, vol. 45, no. 2, pp. 379–404, 2018.
- [17] Cédric Févotte and Jérôme Idier, "Algorithms for nonnegative matrix factorization with the β -divergence," *Neural computation*, vol. 23, no. 9, pp. 2421–2456, 2011.
- [18] V. Leplat, N. Gillis, and A. M. S. Ang, "Blind audio source separation with minimum-volume beta-divergence NMF," *IEEE Transactions on Signal Processing*, vol. 68, pp. 3400–3410, 2020.
- [19] Patrick E McSharry, Gari D Clifford, Lionel Tarassenko, and Leonard A Smith, "A dynamical model for generating synthetic electrocardiogram signals," *IEEE transactions on biomedical engineering*, vol. 50, no. 3, pp. 289–294, 2003.
- [20] S. Peleg and M. Werman, "Fast and robust earth mover's distances," in *IEEE Int. Conf. Computer. Vision.*, 2009, pp. 460–467.
- [21] Ingrid Daubechies, Yi (Grace) Wang, and Hau-Tieng Wu, "Conceft: concentration of frequency and time via a multitapered synchrosqueezed transform," *Philosophical Transactions of the Royal Society A: Mathematical, Physical and Engineering Sciences*, vol. 374, no. 2065, Mar 2016.
- [22] Haizhao Yang, "Statistical analysis of synchrosqueezed transforms," *Applied and Computational Harmonic Analysis*, vol. 45, no. 3, pp. 526–550, 2018.
- [23] Duong Hong Pham and Sylvain Meignen, "High-order synchrosqueezing transform for multicomponent signals analysis-with an application to gravitational-wave signal," *IEEE Trans. Signal Processing*, vol. 65, no. 12, pp. 3168–3178, 2017.
- [24] Antoine Liutkus, Fabian-Robert Stöter, Zafar Rafii, Daichi Kitamura, Bertrand Rivet, Nobutaka Ito, Nobutaka Ono, and Julie Fontecave, "The 2016 signal separation evaluation campaign," in *International conference on latent variable analysis and signal separation*. Springer, 2017, pp. 323–332.